Helically chiral NHC-gold(I) complexes: synthesis, chiroptical properties and electronic features of the [5]helicene-imidazolylidene ligand

Etienne S. Gauthier,[a] Marie Cordier,[a] Vincent Dorcet,[a] Nicolas Vanthuyne,[b] Ludovic Favereau,[a] J. A. Gareth Williams,[c] and Jeanne Crassous*[a]

[a] Dr. Etienne S. Gauthier, Marie Cordier, Dr. Vincent Dorcet, Dr. Ludovic Favereau, Dr. Jeanne Crassous
Univ Rennes, CNRS, ISCR - UMR 6226,
F-35000 Rennes, France.
E-mail: jeanne.crassous@univ-rennes1.fr

[b] Dr. Nicolas Vanthuyne
Aix Marseille University, CNRS Centrale Marseille, iSm2, 13284 Marseille, France.

[c] Prof. J. A. Gareth Williams
Department of Chemistry, Durham University, Durham, DH1 3LE, U.K.

Supporting information for this article is given via a link at the end of the document.

Abstract: We describe the preparation of helically chiral gold(I) complexes bearing a [5]helicenic-N-heterocyclic carbene ligand. They were successfully obtained as enantiopure compounds by semi-preparative chiral HPLC and their structural, chiroptical and photophysical properties were subsequently investigated. Notably, strong electronic circular dichroism, dual emission from singlet and triplet states, with the timescale of the latter up to the millisecond range at room temperature, and moderate circularly phosphorescence were observed. The σ-donating and π-accepting properties of the constituent helical *ortho*-fused π-conjugated carbene were investigated by classical quantitative analysis of the IR stretching frequencies and NMR characteristics of the corresponding $Ir(CO)_2Cl$ complex and selenourea.

Introduction

For three decades since the isolation of the first free carbene by Arduengo *et al.*,[1] *N*-heterocyclic carbenes (NHCs) have become popular strongly σ-donating ligands in organometallic chemistry, thanks to their ability to form stable carbene-metal bonds.[2] The complexes obtained have been shown to offer applications in homogenous catalysis,[3] medicinal chemistry,[4] and materials science.[5] The highly versatile structure of NHCs enables access to complexes with a plethora of transition metal centers in different coordination modes. For instance, many classes of luminescent M-NHC complexes have been developed that have potential in photonic and optoelectronic devices, in bioimaging and cancer therapy, or as photosensitizers in photoredox catalysis.[6] Among the d^{10} coinage metals, gold(I) gives chemically stable complexes[7] that have been applied as luminescent materials,[6d,e] catalysts,[8] and therapeutic agents.[9]

Recently, organometallic complexes bearing chiral NHC ligands have been increasingly studied, mainly owing to interest in enantioselective catalysis,[10,11] but also for their chiroptical features, *i.e.* Electronic Circular Dichroism (ECD)[11] and Circularly Polarized Luminescence (CPL),[6h,11b,d,e] that are appealing in the development of chiral molecular materials.[12] While several classes of chiral NHC-gold(I) complexes have been developed for asymmetric catalysis,[13] results displaying the use of CPL-active NHC-gold(I) complexes are still limited.[14]

Helicenes are *ortho*-condensed polyaromatic molecules; they possess inherent chirality due to the steric repulsion of their skeleton termini.[15] They are known to display strong chiroptical properties such as huge optical rotation values, strong ECD responses and substantial CPL activity.[15i,j] Our group has recently developed chiral versions of several different classes of organometallic compounds by incorporating helicenes within ligands.[16] Of particular interest are helicene-based NHC ligands which have yielded several types of complexes displaying strong ECD spectra[11a,c] and long-lived circularly polarized phosphorescence.[11b,d,e] Herein, we report the synthesis and the structural characterization of two-coordinate helically chiral [5]helicene-NHC gold(I) complexes with diverse ancillary ligands (chloride **1**, acetylenide **2**, carbazolide **3**, Figure 1). They were prepared using *N*-(3,5-dimethylphenyl)-[5]helicenic-imidazolium salt **6**.H^+ as NHC precursor. The intrinsic electronic properties of the carbenic system (σ-donating and π-accepting) and the influence of the helicenic unit were determined using classical quantitative methods based on IR and NMR spectroscopies applied to appropriate derivatives (*i.e.* $Ir(NHC)(CO)_3Cl$ complexes and selenoureas).[17,18] Finally, the gold(I) complexes were obtained as enantiopure complexes by chiral HPLC (with the exception of **3** which was unstable during the separation) and their chiroptics (optical rotation OR and ECD), emission properties and CPL activity were analyzed.

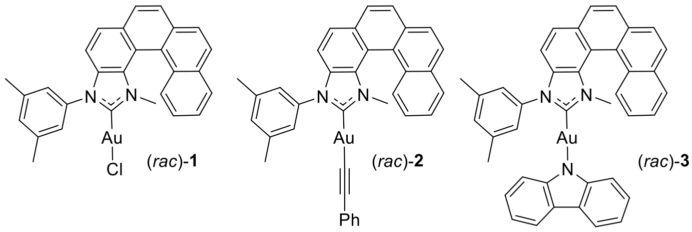

Figure 1. Chemical structures of [5]helicene-NHC-gold(I) complexes **1**, **2** and **3**.

Results and Discussion

Synthesis

First, the imidazolium salt used as NHC proligand was prepared by functionalization of the already reported [5]helicene-imidazole **4**[11b] (Scheme 1). Indeed, the Chan-Lam-Evans coupling of **4** with commercially available 3,5-dimethylphenyl-boronic acid in the presence of copper(II) acetate, triethylamine and activated 4 Å molecular sieves in CH_2Cl_2 under aerobic conditions gave **5** in 83% yield. Then reaction with an excess of methyl iodide in acetonitrile at reflux afforded pentahelicenic imidazolium iodide [(*rac*)-**6**].HI in 89% yield. Finally, the chloride derivative [(*rac*)-**6**].HCl was obtained by anion-metathesis with a Dowex© Cl-exchange resin in 98% yield. The obtention of iodide and chloride imidazolium salts was confirmed by ^1H NMR with the presence of a downfield signal in CD_2Cl_2 (10.77 and 11.86 ppm, respectively), diagnostic of the imidazolium protons.[19] In addition, two singlets were observed between 2.5 and 4 ppm corresponding to the two equivalent CH_3 groups of the 3,5-dimethylphenyl group and of the N-Me group. Characteristic signals of the helicenic unit were also observed; for example, the H^{13} proton appears as a multiplet at 8.34 ppm for (*rac*)-**5** and as a doublet at 8.30 ppm for [(*rac*)-**6**].HI in CD_2Cl_2.

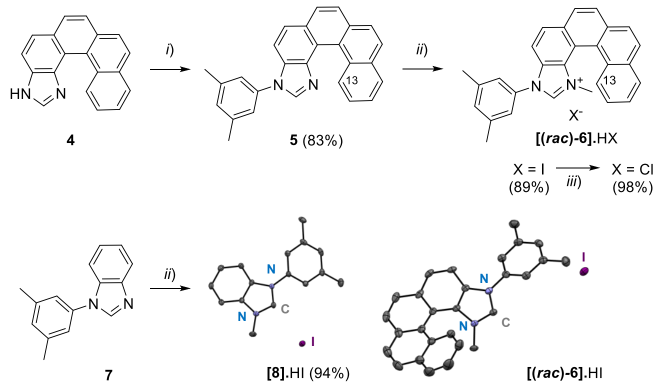

Scheme 1. Preparation of [5]helicene-imidazolium precursors. *i*) 1,3-Dimethylphenylboronic acid, NEt_3, $Cu(OAc)_2$, CH_2Cl_2, 4 Å MS, under air, r.t., 65 h; *ii*) MeI, MeCN, reflux, overnight; *iii*) Dowex Cl-exchange resin, MeOH/Acetone. Yields are indicated under parenthesis.

Single crystals of [(*rac*)-**6**].HI were obtained by slow evaporation of pentane into a dichloromethane solution and were analysed by X-ray crystallography. It crystallizes in the *C*2/*c* centrosymmetric space group and displays a helicity (dihedral angle between the terminal rings) of 47.40°, a typical value for [5]helicenic derivatives.[15a,11b] Both (*M*) and (*P*) helices are present in the crystal and arranged in heterochiral columns along the b axis (see Supplementary Information (SI) for details).

Determination of the Tolmann electronic parameter[20,21] (TEP), based on the average IR-stretching frequency of the carbonyl ligands of [Ir(NHC)Cl(CO)$_2$] complexes, enables the evaluation of the overall electron donation of an NHC ligand. Meanwhile, the measurement of the coupling constant ^1J(C,H) at the precarbenic position of the imidazolium precursor gives the σ-donating ability of the imidazolylidene, as it is inversely proportional to the sigma character of the C-H bond, according to Ganter and co-workers.[22] In addition, the ^{77}Se NMR shift of the related selenium adduct provides clear information about the π-accepting properties of a carbene.[17,18] In order to ascertain the influence of the *ortho*-fused unit on the electronic properties of the NHC, a set of data was also obtained for a model carbene without the helicenic unit. Model salt **[8]**.HI was thus prepared from already known benzimidazole **7**[23] and its X-ray structure was also obtained (Scheme 1).

Complexes (*rac*)-**9** and **10** depicted in Scheme 2 were prepared by a one-pot silver-iridium transmetalation method, using Ag$_2$O then [IrCl(COD)]$_2$ (COD = cyclooctadiene) and obtained in 43% and 72% yield, respectively, from [(*rac*)-**6**].HI and [**8**].HI.[24] The presence of a deshielded signal around 192 ppm in ^{13}C NMR for (*rac*)-**9** and **10** confirmed the presence of the carbenic carbon. These complexes were fully characterized by NMR, HRMS and X-ray analysis (see Figure 2 and Supporting Information, SI).

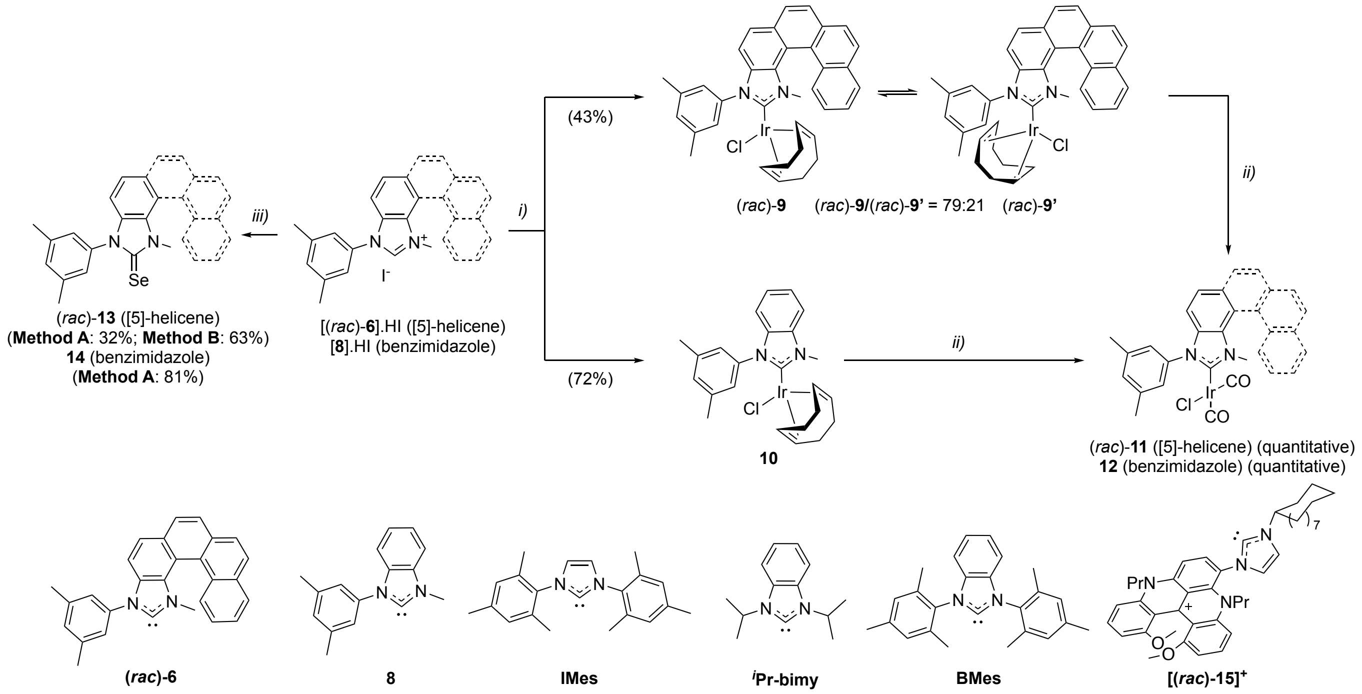

Scheme 2. Preparation of the [5]helicene-imidazolylidene derivatives *i*) a) Ag$_2$O, CH$_2$Cl$_2$, r.t., 2h under Ar in the dark then b) [IrCl(COD)]$_2$, CH$_2$Cl$_2$, r.t., overnight under Ar in the dark; *ii*) CO (balloon), CH$_2$Cl$_2$, r.t., 15 min; *iii*) **Method A**: Se powder, NaHMDS (1.0 M in THF), THF, -78°C to r.t., overnight under Ar or **Method B**: a) Se powder, acetone, 40°C, 15 min under air, b) NEt$_3$, acetone, 60°C, overnight, under air. Yields are indicated in parenthesis.

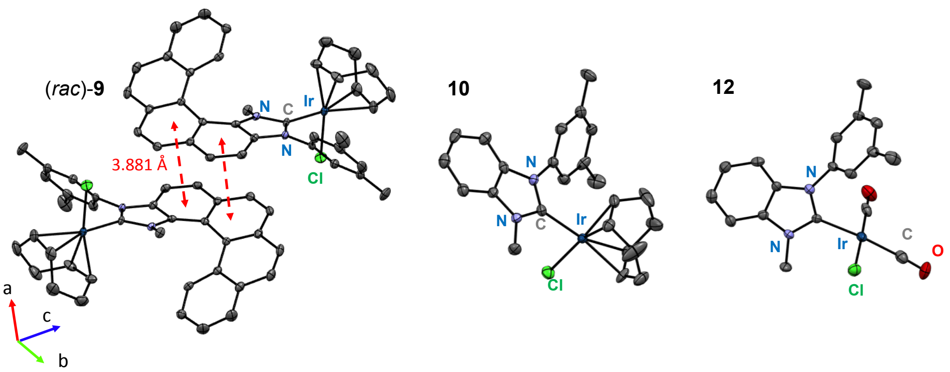

Figure 2. X-ray structures of complexes (*rac*)-**9** (two neighbouring molecules are shown to illustrate their relative disposition), **10** and **12**.

It should be noticed that (*rac*)-**9** was obtained as a mixture of conformers: (*rac*)-**9** and (*rac*)-**9**' with a ratio of 79:21 according to NMR (see Scheme 2 and SI for details). This is in accordance with our earlier work on cyclooctadienyl-iridium(I) complexes bearing a helicenic-NHC.[11c] Indeed, due to the asymmetric nature of the helicenic ligand, the COD ligand can adopt two distinct positions, resulting in the existence of two conformers that are in equilibrium in solution and non-separable by column chromatography. This was fully supported by X-ray crystallography, 2D NMR and theoretical analyses.[11a,c] Single crystals suitable for the analysis of the iridium complexes were obtained by slow evaporation of pentane into a dichloromethane solution. (*Rac*)-**9** and (*rac*)-**10** crystallize in the *P*-1 and *P*bca space groups, respectively (Figure 2). Both structures confirmed the presence of the COD and the chloride ligand coordinated to the pseudo-tetrahedral iridium(I) center with the NHC acting as a monodentate ligand. Regarding the bond lengths, the $C_{carbene}$–Ir bond is slightly longer for the model complex **10** than for the helicenic complex (*rac*)-**9** (2.028 and 2.005 Å, respectively), while no significant difference is observed for the length of the Ir–Cl bond (2.379(2) and 2.361(6) Å, respectively). These values are falling within the range of already published NHC-iridium(I) complexes.[24,25] The helicity of (*rac*)-**9** is 43.52° in a similar range to its pentahelicenic analogues.[11b] It should be noted that the COD ligand is directed toward the helicenic backbone (*P* or *M*) and is the only conformer observed in the crystal, which is in accordance with the data obtained previously.[11c] The supramolecular packing consists of heterochiral columns formed by π-π interactions (3.881 Å) along the a axis (Figure 2). Finally, (*rac*)-**11** and **12** were obtained in quantitative yields by using a balloon filled with carbon monoxide into a solution of (*rac*)-**9** and **10** in CH_2Cl_2 at room temperature for 15 min (Scheme 2).[32] The formation of the [Ir(NHC)Cl(CO)$_2$] complexes was confirmed by IR spectroscopy (ATR) showing the presence of two distinct bands around 2000 cm^{-1}, characteristic of the stretching modes of the two carbonyl ligands. Complex **12** was also characterized by X-ray diffraction, revealing the square planar geometry around the Ir(I) center and the two CO ligands, one of them being *trans* to the NHC monodentate ligand (Figure 2).

Next, deprotonation of [(*rac*)-**6**].HI and [**8**].HI with sodium bis(trimethylsilyl)amide (NaHMDS, as a 1.0 M solution in THF) at -78°C in distilled THF under argon and subsequent trapping of the free carbene with selenium powder afforded selenoureas (*rac*)-**13** and **14** (Scheme 2). Compound **14** was obtained in 81% yield after filtration while (*rac*)-**13** was isolated in 32% yield after column chromatography. Very recently, Nolan and co-workers presented a milder approach to access selenoureas and thioureas by reaction of the imidazolium salt with selenium powder and NEt_3 under air in acetone at 40°C then 60°C overnight.[26] The use of these conditions enabled (*rac*)-**13** to be prepared in 63% yield without any purification. The deshielded signal around 169 ppm in ^{13}C NMR and the observation of one signal in ^{77}Se NMR in d_6-acetone confirmed the presence of the C=Se moiety and the nature of (*rac*)-**13** and **14**.

Determination of the electronic properties of the [5]helicenic carbene and comparative study with known NHCs

The TEP, ^1J(C,H) and ^{77}Se NMR values (in $CDCl_3$ and in d_6-acetone) for (*rac*)-**6** and **8** are gathered in Table 1. Data of already described NHCs (including the well-known **IMes**) were also added for comparison (see structures in Scheme 2).[17] Concerning the donating properties, the coupling constants are similar for (*rac*)-**6** and **8** (222 Hz) indicating that they have comparable σ-donating properties. On the other hand, the substitution pattern of the NHC appears to play a more important role, since the **^{i}Pr-bimy** (without aryl groups) and the **IMes** have a lower and a higher coupling constant (218 and 225 Hz respectively). Interestingly, [(*rac*)-**15**]$^+$ possesses a higher coupling constant (224 Hz) than (*rac*)-**6** owing to the cationic nature of the [4]helicenium arm and its σ-withdrawing properties. Additionally, TEP values for (*rac*)-**6** and **8** were found to fall in the same range as **IMes**, **^{i}Pr-bimy**, **BMes** and [(*rac*)-**15**]$^+$, thus reinforcing the point that the helicenic backbone has no pronounced influence on the donor character of the NHC. The absence of any clear backbone effect on the TEP was already highlighted by Huynh.[17] The influence of the aromatic backbone on the accepting properties was shown by the disparities in the ^{77}Se NMR shifts in d_6-acetone. A clear trend can be established within the values: the **IMes** without backbone has the lower value (35 ppm) followed by helicenium [(*rac*)-**15**]$^+$ (65, 49 ppm) and finally the **^{i}Pr-bimy** (67 ppm). Hence, it seems to indicate that a conjugated backbone has a more pronounced influence on the π-accepting properties than the peripheral aryl groups. Indeed, this is supported by the model carbene **8**, which combines both structural aspects, and has an even higher ^{77}Se shift (113 ppm). Finally, it is confirmed with the [5]helicenic-NHC (*rac*)-**6**, which possesses the highest value (133 ppm) of the series. Including [(*rac*)-**15**]$^+$ in the study highlighted the importance of the position of the helicene with respect to the carbene: higher π-accepting character has been obtained with a fully *ortho*-fused helicenic NHC in comparison with an *N*-substituted helicenyl NHC. In the end, due to an easier delocalization of the electron density over the helicenic unit, it can be easily understood that the *ortho*-fused helicenic carbene is a better π-acceptor than the other carbenes.

Table 1. Electronic parameters of the studied NHCs

NHC	^1J(C,H) (Hz)^a	δ(^{77}Se) (ppm)^b		TEP [$\nu_{average}$, CO] (cm^{-1})^c
		In $CDCl_3$	In d_6-acetone	
(*rac*)-6	222	106	133	2053 [2025.3]
8	222	91	113	2054 [2027.3]
IMes[21]	225	27	35	2051
^{i}Pr-bimy[21]	218	—	67	2054
BMes[21]	—	—	—	2052
[(*rac*)-15]$^+$[20]	224	—	65, 49^d	2055

^{a} Measured on the corresponding imidazolium precursor in $CDCl_3$; ^{b} Measured on the corresponding selenoureas; ^{c} Measured on the corresponding [NHC-Ir(CO)$_2$Cl] complex in CH_2Cl_2, TEP was calculated from the average value of the CO bands' frequency (in brackets for the first two complexes) following Nolan *et al.* : TEP (cm^{-1}) = $0.8475\nu_{average,\ CO}$(cm^{-1}) + 336.2 (cm^{-1}).[21,22,26] ; ^{d} The two resonances arise from the presence of two atropoisomers.[14b]

Preparation and characterization of the enantiopure [5]helicene-imidazolylidene-gold(I) complexes

It should be noted that the helical chirality (*P*/*M*) is not stable in the [5]helicene-imidazole derivatives **4** and **5** as previously demonstrated.[11b] After the quaternarization, the N-Me group inside the helical groove hampers the inversion of the helix thus resulting in a configurationally stable helicene [(*rac*)-**6**].HX (X = I, Cl). However, due to their cationic nature, the enantiomeric resolution using chiral HPLC is not straightforward under conventional methods. The salts were therefore subjected to gold(I) metalation in their racemic forms. The metalation was conducted using [(*rac*)-**6**].HCl following a procedure that requires neither inert atmosphere nor strong base.[27] [(*Rac*)-**6**].HCl was stirred with 1 equivalent of [AuCl(Me_2S)] and a base (K_2CO_3) in acetone at 60°C for one hour in the dark and under air. After filtration over silica gel and precipitation, the desired NHC-Au-Cl complex (*rac*)-**1** was isolated as a stable white solid in 94% yield. Then, (*rac*)-**1** was used as a common precursor to prepare the phenyl-acetylide and the carbazolide derivatives, (*rac*)-**2** and (*rac*)-**3**, respectively. (*Rac*)-**2** was prepared by a ligand-exchange reaction by mixing the gold chloride (*rac*)-**1**, phenylacetylene and K_2CO_3 in methanol at 70°C for 2h under air and was obtained in 81% yield after filtration over basic alumina and precipitation.[28] (*Rac*)-**3** was prepared by mixing (*rac*)-**1**, 9H-carbazole and NaO^{t}Bu in distilled THF under argon at 70°C overnight and was obtained in 69% yield after filtration over basic alumina and precipitation (Scheme 3).

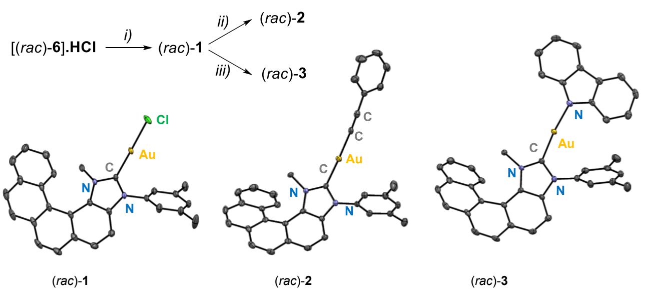

Scheme 3. Preparation of the helicenic-gold(I) complexes **1**-**3**. *i)* [AuCl(Me_2S)], K_2CO_3, Acetone, 60°C, 1h, in the dark under air, 94%; *ii)* phenylacetylene, K_2CO_3, MeOH, 70°C, 2h, under air, 81%; *iii)* 9H-carbazole, NaO^{t}Bu, distilled THF, 70°C, overnight under argon, 69%. X-ray structures of (*rac*)-**1**, (*rac*)-**2** and (*rac*)-**3**. CCDC numbers and crystallographic details are in the SI. Hydrogens have been omitted for clarity. Only one enantiomer is shown.

All the complexes were fully characterized using 1D and 2D NMR. ^{13}C NMR signals for the expected carbenic carbons were observed around 180-190 ppm in line with the literature.[8,29] The absence of any signal around 11-12 ppm in the ^{1}H NMR spectra confirmed the consumption of the imidazolium precursor, while the protons from the [5]helicenic unit were observed, notably H^{13} (see numbering in Scheme 1) which appears as a doublet at 8.32 ppm for (*rac*)-**1**, as a multiplet at 8.36 ppm for (*rac*)-**2** and as a doublet at 8.43 ppm for (*rac*)-**3** (see SI for further details). Single crystals suitable for X-ray characterization of the complexes **1**-**3** were obtained which confirmed their monomeric nature (Scheme 3). They all crystallized in centrosymmetric space groups, *i.e.* *C*2/c, *P*-1 and *P*2_1/*c* for (*rac*)-**1**, (*rac*)-**2** and (*rac*)-**3**, respectively, with helicities close to 50° in accordance with other [5]helicenic derivatives (see Table S1 for details).[11b,15a] Regardless of the ancillary ligand, the geometry around the gold(I) center is nearly linear (dihedral angles $C_{carbene}$-Au-Y between 173.24-178.30° where Y = Cl, C or N) in accordance with already reported two-coordinate NHC-Au(I) complexes.[6d,29] It should be mentioned that none of the complexes exhibit metallophilic interactions in the solid state due to the distance between two neighboring gold centers being too long (3.893 Å for (*rac*)-**1** and 4.026 Å for (*rac*)-**3**, with respect to the van der Waals radius of the gold atom established at 1.66 Å), except for (*rac*)-**2** which has a shortest gold-gold distance of 3.567 Å, sufficiently short to infer weak aurophilic interactions.[6d,30] The absence of strong metallophilic interactions is probably related to the bulkiness of the helical *ortho*-fused unit in addition to the presence of a moderately bulky aryl substituent attached to the NHC ring.[30b]

The chiral HPLC separation of the enantiomers of **1**, **2** and **3** was then examined. Complexes **1** and **2** were eluted on a Chiralpak IH column and a Chiralpak IB column respectively to afford isolated (*P*) and (*M*) enantiomers with excellent enantiomeric excesses (*ee* values > 97.5 %, see SI for details). The carbazolide complex **3** was eluted on a Chiralpak IA column but the compound decomposed during the separation, forming an impurity visible on the chromatograms (see SI). It suggests that the Au-$N_{carbazolide}$ bond in NHC-gold-carbazolide complexes is only moderately stable over stationary phases (silica gel or basic alumina). Thus, only the photophysical and chiroptical properties of complexes **1** and **2** were investigated.

Photophysical properties

The UV/Vis absorption spectra of (*rac*)-**1** and (*rac*)-**2** were recorded in CH_2Cl_2 at concentrations around 10^{-4} M (Figure 3a). Both complexes exhibit intense and highly structured bands < 330 nm attributable to the extended π-helical unit. For example, **1** exhibits well-resolved bands at λ = 265 (ε = 36 100), 290 (41 700), 298 (4000) and 316 nm (33 700 M^{-1} cm^{-1}). At lower energies, there is a shoulder at 352 nm (2400 M^{-1} cm^{-1}) and a pair of weaker bands at 370 (2500 M^{-1} cm^{-1}) and 388 nm (2200 M^{-1} cm^{-1}). The spectrum of the acetylenide derivative **2** is essentially identical to that of **1** in this region, whilst it has slightly augmented absorption at higher energies, i.e. around 280 nm, owing to the presence of the phenylacetylene π-π* transitions which usually occur at λ < 340 nm.

Both complexes are luminescent in CH_2Cl_2 solution at room temperature (Figure 4 and Table S3). In deoxygenated solution, they display two well-separated sets of vibrationally structured bands, with the 0,0 vibrational components at 393 and about 515 nm. In air-equilibrated solution, only the higher-energy set is observed. This behaviour is suggestive of dual emission from singlet and triplet states, with the latter being quenched efficiently by dissolved molecular oxygen. Such an assignment is reinforced by time-resolved measurements that reveal a lifetime of the lower-energy band of around 1 ms (0.8 ms for **1** and 1.5 ms for **2**); lifetimes of this order are typical of triplet states. With such a long triplet lifetime, considerable vibrational quenching would be anticipated, and indeed, at 77 K, the intensity of the phosphorescence band drastically increases, dwarfing the fluorescence. The phosphorescence lifetimes under these conditions are increased by more than an order of magnitude to 52 and 19 ms for **1** and **2** respectively. The vibronic progression of both the fluorescence and phosphorescence bands at room temperature is around 1350 cm^{-1} for both complexes, no doubt corresponding to C=C stretching modes of the helicene and indicative of an excited state of primarily ligand-centred character.

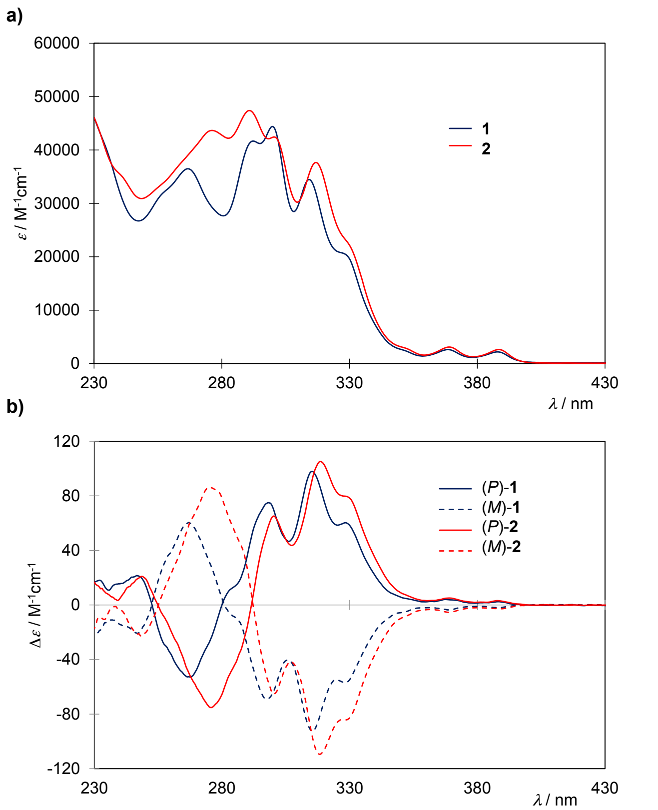

Figure 3. a) UV-Vis absorption and b) ECD spectra of enantiopure complexes (*P*) and (*M*)-**1** (blue lines) and **2** (red lines) recorded in CH_2Cl_2 at around 10^{-4} M.

The main difference between **1** and **2** is the higher overall quantum yield of the latter: the values are 0.50 and 1.6 % respectively in deoxygenated solution. Moreover, the relative intensity of the phosphorescence (P) compared to the fluorescence (F) is higher in the acetylide derivative **2**: the ratio of the integrated intensities P/F is approximately 1.9 and 4.5 for **1** and **2** respectively (compare Figure 4 and Figure S32). Coupled with the phosphorescence lifetime of **2** being around double that of **1**, it thus appears that the augmented quantum yield of **2** is associated with less severe non-radiative decay of the triplet state. Chloride to acetylide metathesis has previously been found to have such an effect in other gold complexes, often attributed to the higher ligand field strength of the acetylide helping to ensure that potentially deactivating d-d states are kept at bay, to high energy.[31]

It is informative to compare the behaviour of **1** and **2** with other Au(I) NHC complexes. Non-helicenic NHC complexes that do not have extended conjugation in their ligands exhibit only phosphorescence,[28] whilst the recently reported helicenic complex [(*rac*)-**15**]Au^{I}Cl.PF_6 (Scheme 2) – featuring a highly extended conjugated system – shows only fluorescence in the red region, reminiscent of the *N*-[4]helicenium-imidazolium ligand.[14b] The dual emission – phosphorescence *and* fluorescence – of **1** and **2** places them between these two extremes. Observation of phosphorescence requires spin-orbit coupling to be sufficiently efficient not only to promote the formally forbidden $T_1 \rightarrow S_0$ radiative process, but also to facilitate the $S_1 \rightarrow T_1$ intersystem crossing. It has been found in other systems {e.g. with Os(II), Pt(II) and Ir(III)} that, as the conjugated ligand system becomes more extended, the associated π orbitals increase in energy and mix less efficiently with metal orbitals, leading to more purely ligand-centred character to the excited state and thus to less efficient spin-orbit coupling.[32] Fluorescence then becomes more likely to be able to compete with intersystem crossing. Such an effect may be at work in the present case, though it must be acknowledged that spin-orbit coupling pathways are complex and may also be heavily influenced by, for instance, the relative energies of higher-lying singlet states relative to T_1.[33]

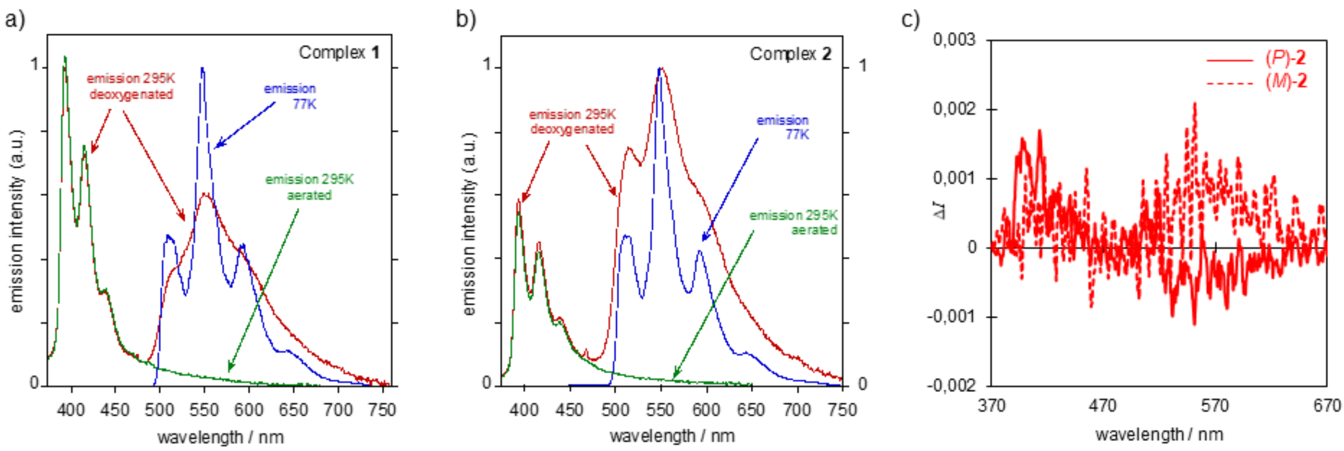

Figure 4. Emission spectra of **1** and **2** (left and centre panels respectively) in deoxygenated and air-equilibrated CH_2Cl_2 at 295 K (red and green lines respectively, plotted on the same intensity scale, λ_{ex} = 350 nm) and in EPA at 77 K (blue lines, maximum intensity normalised to that of the deoxygenated 295 K spectrum). EPA = diethyl ether / isopentane / ethanol (2:2:1 v/v). Right panel: CPL spectra of (*M*) and (*P*)-**2** measured at 298 K in degassed CH_2Cl_2, λ_{exc} = 345 nm (15 and 30 scans respectively).

Chiroptical properties

The chiroptical properties (OR, ECD, and CPL) of **1** and **2** were investigated in CH_2Cl_2. The molar rotation values at 25°C were similar for both complexes, around 5-6 × 10^3 which is quite typical for [5]helicenic complexes.[11b] The combination of the polarimetry (sign of the optical rotations) with ECD spectroscopy (alternation of bands with opposite signs, characteristic of a helicenic system, Figure 3b) helped to assign the (*P*)-(+) / (*M*)-(-) absolute stereochemistry of each enantiomer, by analogy with other complexes. The structured profile observed in UV-vis spectroscopy is evident also in ECD, confirming the strong involvement of the helically chiral *ortho*-fused unit in the observed polarized and unpolarized excitations of the complexes. For example, (*P*)-**1** exhibits a first positive band at 247 nm ($\Delta\varepsilon$ = +21 $M^{-1}cm^{-1}$) followed by a negative one at 268 nm (-54). Next, the complex displays a series of positive and structured bands at 298 (+75), 315 (+98) and 328 (+60). Finally, two bands of lowest energies can be found at 369 (+4) and 388 nm (+2). The spectrum of (*P*)-**2** is identical in terms of the alternation of bands with the exception of the band at 266 nm which appears slightly red-shifted (about 10 nm) and more intense ($\Delta\varepsilon$ = -75 $M^{-1}cm^{-1}$). For comparison, the gold(III) complex [(*P*)-**15**]$Au^{III}L.(PF_6)_2$ (L = 2,6-diphenylpyridine) recently described[14b] displays ECD bands in acetonitrile in the UV region diagnostic of helicenic derivatives —237 nm ($\Delta\varepsilon$ = +23 $M^{-1}cm^{-1}$), 287 nm (+52), 320 nm (+21)— in addition to observable bands in the red region of somewhat lower intensity —600 nm ($\Delta\varepsilon$ = + 8 $M^{-1}cm^{-1}$). The lower intensities of [(*P*)-**15**]$Au^{III}L.(PF_6)_2$ with respect to (*P*)-**1** can be explained by the smaller length of the helical unit. It proved possible to measure weak CPL signals for the phosphorescence of enantiopure complexes of **2** in deoxygenated solution (g_{lum} ~ +1 × 10^{-3} and -1 × 10^{-3} for (*M*)-**2** and (*P*)-**2**, respectively, at λ_{em} = 550 nm, see Figure 4). The weakness of the detected signal arises in part from the low quantum yields and from inefficient interaction between the helicenic and the metallic part. Furthermore, it can be seen from the higher-energy region of the CPL spectra that the fluorescence displays no CPL activity, at least within the sensitivity of our apparatus.

Conclusion

In conclusion, we have reported helically chiral [5]helicenic-imidazolylidene gold(I) complexes bearing various ancillary ligands. Using a straightforward synthetic approach, the targeted complexes were obtained in good yields and were fully characterized, notably using X-ray diffraction. Additionally, en route to the complexes, the electronic properties of the constituent carbene with an *ortho*-fused π-conjugated system as backbone were highlighted. These quantitative analyses revealed that the presence of the helicenic backbone impacts only the accepting properties of the NHC, with no clear effect on the donating properties. Except for the carbazolide derivative, the NHC-gold(I) complexes exhibit high chemical stability on chiral stationary phases and were separated into their enantiomers by semi-preparative chiral HPLC. Their chiroptical and photophysical properties revealed their strong ECD activity due to the presence of the [5]helicenic unit as well as dual luminescence from singlet and triplet states at room temperature together with long lifetimes for the triplet phosphorescence. Finally, CPL activity could be clearly detected for complexes (*P*) and (*M*)-**2**. Considering the good chemical and configurational stability of these chiral NHC-gold(I), this work paves the way to further developments of gold complexes or assemblies.

Acknowledgements

We thank the Centre National de la Recherche Scientifique (CNRS) and the University of Rennes. This work was supported by the Agence Nationale de la Recherche (ANR-16-CE07-0019 “Hel-NHC” grant). Dr. Clément Orione (ScanMat-ISCR), Dr. Antoine Vacher (ISCR), Pr. François-Hugues Porée (ISCR) are acknowledged for their assistance respectively with NMR measurements, IR measurements and for reactions with carbon monoxide.

Keywords: helicene, N-heterocyclic carbene, gold(I), organometallic, electronic circular dichroism, CPL

[1] A. J. Arduengo, R. L. Harlow, M. Kline, *J. Am. Chem. Soc.* **1991**, *113*, 361–363.

[2] a) D. Bourissou, O. Guerret, F. P. Gabbai, G. Bertrand, G. *Chem. Rev.* **2000**, *100*, 39-91; b) S. Díez-González (Ed.), *N-Heterocyclic Carbenes: From Laboratory Curiosities to Efficient Synthetic Tools*; RSC: Cambridge, UK; **2011**; c) M. N. Hopkinson, C. Richter, M. Schedler, F. Glorius, *Nature* **2014**, *510*, 485–496.

[3] a) S. Díez-González, N. Marion, S. P. Nolan, *Chem. Rev.* **2009**, *109*, 3612–3676; b) V. César, S. Bellemin-Laponnaz, L. H. Gade, *Chem. Soc. Rev.* **2004**, *33*, 619–636; c) F. Wang, L.-J. Liu, W. Wang, S. Li, M. Shi, *Coord. Chem. Rev.* **2012**, *256*, 804–853; d) D. Zhao, L. Candish, D. Paul, F. Glorius, *ACS Catal.* **2016**, *6*, 5978–5988.

[4] K. M. Hindi, M. J. Panzner, C. A. Tessier, C. L. Cannon, W. J. Youngs, *Chem. Rev.* **2009**, *109*, 3859–3884.

[5] a) M. Mercs, M. Albrecht, *Chem. Soc. Rev.* **2010**, *39*, 1903–1912; b) R. Visbal, M.C. Gimeno, *Chem. Soc. Rev.* **2014**, *43*, 3551–3574; c) C. A. Smith, M. R. Narouz, P. A. Lummis, I. Singh, A. Nazemi, C. -H. Li, C. M. Crudden, *Chem. Rev.* **2019**, *119*, 4986–5056.

[6] a) Y. Unger, D. Meyer, T. Strassner, *Dalton Trans*. **2010**, *39*, 4295–4301; b) T. Sajoto, P. I. Djurovich, A. Tamayo, M. Yousufuddin, R. Bau, M. E. Thompson, R. J. Holmes, R. S. Forrest, *Inorg. Chem*. **2005**, *44*, 7992–8003; c) S. U. Son, K. H. Park, Y.-S. Lee, B. Y. Kim, C. H. Choi, M. S. Lah, Y. H. Jang, D.-J. Jang, Y. K. Chung, *Inorg. Chem*. **2004**, *43*, 6896–6898; d) H. M. J. Wang, C. Y. L. Chen, I. J. B. Lin, *Organometallics* **1999**, *18*, 1216–1223; e) D. Di, A. S. Romanov, L .Yang, J. M. Richter, J. P. H. Rivett, S. Jones, T. H. Thomas, M. A. Jalebi, R. H. Friend, M. Linnolahti, M. Bochmann, D. Credgington, *Science* **2017**, *356*, 159–163; f) R. Hamze, S. Shi, S. C. Kapper, D. S. M. Ravinson, L. Estergreen, M. -C. Jung, A. C. Tadle, R. Haiges, P. I. Djurovich, J. L. Peltier, R. Jazzar, G. Bertrand, S. E. Bradforth, M. E. Thompson, *J. Am. Chem. Soc.* **2019**, *141*, 21, 8616–8626; g) R. Hamze, J. L. Peltier, D. Sylvinson, M. Jung, J. Cardenas, R. Haiges, M. Soleilhavoup, R. Jazzar, P. I. Djurovich, G. Bertrand, M. E. Thompson, *Science* **2019**, *363*, 601–606; h) M. Deng, N. F. M. Mukthar, N. D. Schley, G. Ung. *Angew. Chem. Int. Ed.* **2020**, *59*, 1228–1231; i) H. Tatsuno, *et al.* *Angew. Chem. Int. Ed.* **2020**, *59*, 364–372; j) P. V. Simpson, M. Falasca, M. Massi, *Chem. Commun.* **2018**, *54*, 12429–12438.

[7] a) J. C. Y. Lin, R. T. W. Huang, C. S. Lee, A. Bhattacharyya, W. S. Hwang, I. J. B. Lin, Chem. Rev. **2009,** *109*, 3561–3598S; b) Gaillard, A. M. Z. Slawin, S. P. Nolan, *Chem. Commun.* **2010**, *46*, 2742-2744.

[8] a) T. Wurm, A. Mohamed Asiri, A. S. K. Hashmi, in *N-Heterocyclic Carbenes* (Ed.: S.P. Nolan), Wiley-VCH Verlag GmbH & Co. KGaA, Weinheim, Germany, **2014**, pp. 243–270; b) S. P. Nolan, *Acc. Chem. Res.* **2011**, *44*, 91–100.

[9] M. Mora, M. C. Gimeno, R. Visbal, *Chem. Soc. Rev.* **2019**, *48*, 447–462.

[10] a) F. Wang, L. Liu, W. Wang, S. Li, M. Shi, *Coord. Chem. Rev.* **2012**, *256*, 804–853; b) D. Janssen-Müller, C. Schlepphorst, F. Glorius, *Chem. Soc. Rev.* **2017**, *46*, 4845–4854.

[11] a) N. Hellou, C. Jahier-Diallo, O. Baslé, M. Srebro-Hooper, L. Toupet, T. Roisnel, E. Caytan, C. Roussel, N. Vanthuyne, J. Autschbach, M. Mauduit, J. Crassous, *Chem. Comm.* **2016**, *52*, 9243–9246; b) N. Hellou, M. Srebro-Hooper, L. Favereau, F. Zinna, E. Caytan, L. Toupet, V. Dorcet, M. Jean, N. Vanthuyne, J. A. G. Williams, L. Di Bari, J. Autschbach, J. Crassous, *Angew. Chem. Int. Ed.* **2017**, *56*, 8236–8239; c) N. Hafedh, L. Favereau, E. Caytan, T. Roisnel, M. Jean, N. Vanthuyne, F. Aloui, J. Crassous˙ *Chirality* **2019**, *31*, 1005–1013 ; d) A. Macé, N. Hellou, J. Hammoud, C. Martin, E. S. Gauthier, L. Favereau, T. Roisnel, E. Caytan, G. Nasser, N. Vanthuyne, J. A. G. Williams, F. Berrée, B. Carboni, J. Crassous, *Helv. Chim. Acta* **2019**, *102*, e1900044; e) E. S. Gauthier, L. Abella, N. Hellou, B. Darquié, E. Caytan, T. Roisnel, N. Vanthuyne, L. Favereau, M. Srebro-Hooper, J. A. G. Williams, J. Autschbach, J. Crassous, *Angew. Chem. Int. Ed.* **2020**, *59*, 8394–8400.

[12] For other examples of helicene-NHCs see: a) I. G. Sanchez, M. Samal, J. Nejedly, M. Karras, J. Klivar, J. Rybacek, M. Budesinsky, L. Bednarova, B. Seidlerova, I. G. Stara, I. Stary, *Chem. Commun.* **2017**, *53*, 4370–4373; b) M. Karras, M. Dąbrowski, R. Pohl, J. Rybáček, J. Vacek, L. Bednárová, K. Grela, I. Starý, I. G. Stará, B. Schmidt, *Chem. Eur. J.* **2018**, *24*, 10994–10998; c) P. Morgante, B. Captain, C. D. Chouinard, R. Peverati, N. Takenaka, *Tetrahedron Lett.*, **2020**, *61*, 152143.

[13] M. Michalak, W. Kośnik, *Catalysts* **2019**, *9*, 890.

[14] a) J. Yang, K. Li, J. Wang, S. Sun, W. Chi, C. Wang, X. Chang, C. Zou, W. To, M. Li, X. Liu, W. Lu, H. Zhang, C. Che, Y. Chen, *Angew. Chem. Int. Ed.* **2020**, *59*, 6915–6922; b) R. Tarrieu, I. Hernandez Delgado, F. Zinna, V. Dorcet, S. Colombel-Rouen, C. Crévisy, O. Basle, J. Bosson, J. Lacour, *Chem. Commun.* **2021**, *57*, 3793–3796.

[15] a) C.-F. Chen, Y. Shen, 'Helicene Chemistry: From Synthesis to Applications'; Springer Berlin Heidelberg: Berlin, Heidelberg, **2017**; b) Y. Shen, C. F. Chen, *Chem Rev*. **2012**, *112*, 1463–1535; c) M. Gingras, *Chem. Soc. Rev.* **2013**, *42*, 1051–109; d) P. Aillard, A. Voituriez and A. Marinetti, *Dalton Trans.* **2014**, *43*, 15263–1527828; e) J. Bosson, J. Gouin and J. Lacour, *Chem. Soc. Rev.* **2014**, *43*, 2824-2840; f) K. Dhbaibi, L. Favereau, J. Crassous, *Chem. Rev.* **2019**, *119*, 8846–8953; g) I. G. Stara and I. Stary, *Acc. Chem. Res.* **2020**, *53*, 144-158; h) H. Isla, J. Crassous, *C. R. Chimie* **2016**, *19*, 39–49; i) W.-L. Zhao, M. Li, H.-Y. Lu, C.-F. Chen, *Chem. Commun.* **2019**, *55*, 13793-13803; j) J. Crassous in "Circularly Polarized Luminescence of Isolated Small Organic Molecules", T. Mori (ed.), Springer, **2020**, chap. 4, pp 53-97

[16] a) N. Saleh, C. S. Shen and J. Crassous, *Chem. Sci.* **2014**, *5*, 3680–3694; b) J.-K. Ou-Yang, J. Crassous*, Coord. Chem. Rev.* **2018**, *376*, 533–547; c) E. S. Gauthier, R. Rodríguez, J. Crassous, *Angew. Chem. Int. Ed.* **2020**, *59*, 22840–22856.

[17] H. V. Huynh, *Chem. Rev.* **2018**, *118*, 9457–9492.

[18] D. J. Nelson, S. P. Nolan, *Chem. Soc. Rev.* **2013**, *42*, 6723–6753.

[19] H. V. Huynh, T. T. Lam, H. T. T. Luong, *RSC Adv.* **2018**, *8*, 34960–34966.

[20] T. Dröge, F. Glorius, *Angew. Chem. Int. Ed.* **2010**, *49*, 6940–6952.

[21] R. A. Kelly III, H. Clavier, S. Giudice, N. M. Scott, E. D. Stevens, J. Bordner, I. Samardjiev, C. D. Hoff, L. Cavallo, S. P. Nolan, *Organometallics* **2008**, *27*, 202–210.

[22] K. Verlinden, H. Buhl, W. Frank, C. Ganter, *Eur. J. Inorg. Chem.* **2015**, *2015*, 2416–2425.

[23] A. Klapars, J. C. Antilla, X. Huang, S. L. Buchwald, *J. Am. Chem. Soc.* **2001**, *123*, 7727–7729.

[24] A. R. Chianese, A. Mo, D. Datta, *Organometallics* **2009**, *28*, 465–472.

[25] A. R. Chianese, X. Li, M. C. Janzen, J. W. Faller, R. H. Crabtree, *Organometallics* **2003**, *22*, 1663–1667.

[26] N. V. Tzouras, F. Nahra, L. Falivene, L. Cavallo, M. Saab, K. Van Hecke, A. Collado, C. J. Collett, A. D. Smith, C. S. J. Cazin, S. P. Nolan, *Chem. Eur. J.* **2020**, *26*, 4515–4519.

[27] A. Collado, A. Gómez-Suárez, A. R. Martin, A. M. Z. Slawin, S. P. Nolan, *Chem. Commun.* **2013**, *49*, 5541.

[28] A. A. Penney, G. L. Starova, E. V. Grachova, V. V. Sizov, M. A. Kinzhalov, S. P. Tunik, *Inorg. Chem.* **2017**, *56*, 14771–14787.

[29] a) H. M. J. Wang, C. S. Vasam, T. Y. R. Tsai, S.-H. Chen, A. H. H. Chang, I. J. B. Lin, *Organometallics* **2005**, *24*, 486–493; b) J. A. Garg, O. Blacque, J. Heier, K. Venkatesan, *Eur. J. Inorg. Chem.* **2012**, *2012*, 1750–1763.

[30] a) P. Pyykkö, *Chem. Rev.***1997**, 97,597−636; b) A. Wuttke, M. Feldt, R. A. Mata, *J. Phys. Chem. A* **2018**, *122*, 34, 6918–6925. autres

[31] a) K. H. Wong, K. K. Cheung, M. C.-W. Chan, C.-M. Che, *Organometallics* **1998**, *17*, 3505–3511; b) R. R. Parker, D. Liu, X. Yu, A. C. Whitwood, W. Zhu, J. A. G. Williams, Y. Wang, J. M. Lynam, D. W. Bruce, *J. Mater. Chem. C* **2021**, *9*, 1287–1302.

[32] a) Y.-L. Chen, S.-W. Li, Y. Chi, Y.-M. Cheng, S.-C. Pu, Y.-S. Yeh, P.-T. Chou, *ChemPhysChem* **2005**, *6*, 2012–2017; b) P.-T. Chou, Y. Chi, M.-W. Chung, C.-C. Lin, *Coord. Chem. Rev.* **2011**, *255*, 2653–2665; c) D. M. Kozhevnikov, V. N. Kozhevnikov, M. Z. Shafikov, A. N. Prokhorov, D. W. Bruce, J. A. G. Williams, *Inorg. Chem.* **2011**, *50*, 3804–3815

[33] H. Yersin, A. F. Rausch, R. Czerwieniec, T. Hofbeck, T. Fischer, *Coord. Chem. Rev.* **2011**, *255*, 2622–2652.

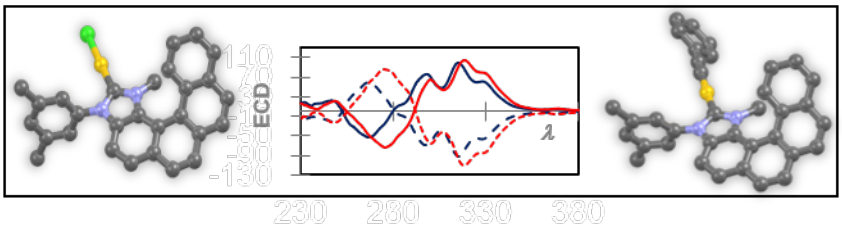

The golden twist: Monodentate [5]helicene-imidazolylidene gold(I) complexes were prepared in good yields and structurally characterized. Benefiting from the presence of the configurationally stable [5]helicenic unit, they exhibit appealing chiroptical features, such as strong circular dichroism, moderate circularly polarized phosphorescence and dual emission with phosphorescence lifetimes up to the millisecond range.

Institute and/or researcher Twitter usernames: @EGA_Chem, @JeanneCrassous, @chimie_ISCR